# The effect of small concentrations of sulfur on the plasticity of zirconium alloys at intermediate temperatures

Franck Ferrer, Alain Barbu, Thierry Bretheau, Jérôme Crépin, François Willaime, Daniel Charquet

# The Effect of Small Concentrations of Sulfur on the Plasticity of Zirconium Alloys at Intermediate Temperatures

*Franck Ferrer,*[1] *Alain Barbu,*[2] *Thierry Bretheau,*[3] *Jérôme Crépin,*[3] *François Willaime,*[4] *and Daniel Charquet*[5]

**ABSTRACT:** The effect of the addition of some ten ppm sulfur to α-zirconium and Zr-1 %Nb-0.13%O alloy is investigated. A strong hardening effect is demonstrated. The hardening effect appears at about 100° C and is maximal around 400°C. Based on creep and constant strain-rate tests, and scanning electron microscopy and transmission electron microscopy observations, it is concluded that sulfur modifies the deformation kinetics, with no change in the deformation mechanisms. The sulfur effect is viscous-like. The screening of all the potential controlling mechanisms allows us to postulate a sulfur segregation involving modifications of the dislo-cation core structure and then of the dislocation mobility. *Ab initio* simulations are consistent with this hypothesis.

**KEYWORDS:** mechanical behavior, sulfur, deformation mechanisms, temperature, dislocation, Zr alloys, oxygen, hardening effect

## Introduction

The addition of 25 weight ppm sulfur is enough to reduce by a factor of three the creep rate of zirconium alloys at 400°C (Fig. 1) as demonstrated at Framatome ANP [1]. Such a strong effect by such a small concentration suggests that sulfur acts directly on the mechanisms controlling the deformation kinetics. At the beginning of the present work, these mechanisms were still poorly identified, and they had to be specified first. Sulfur provides a very powerful probe to test the validity of these deformation mechanisms. By considering all the potential controlling mechanisms and comparing them to the measurements and observations performed at all the reachable scales, most mechanisms could be eliminated, and the most probable controlling mechanism was identified.

[1] Ph.D Student, Laboratoire de Mécanique des Solides and Laboratoire des Solides Irradiés, Ecole Polytechnique, 91128 Palaiseau, France, now researcher at CESMAN-DCN, Indret, 44620 La Montagne, France.

[2] Senior Researcher, Laboratoire des Solides Irradiés, Ecole Polytechnique, 91128 Palaiseau, France.

[3] Senior Researchers, Laboratoire de Mécanique des Solides, Ecole Polytechnique, 91128 Palaiseau, France.

[4] Senior Researcher, Service de Recherches de Métallurgie Physique, CEA/Saclay, 91191 Gif/Yvette, France.

[5] Senior Engineer, Cézus Framatome ANP, Centre de Recherche d'Ugine, 73403 Ugine Cedex, France.

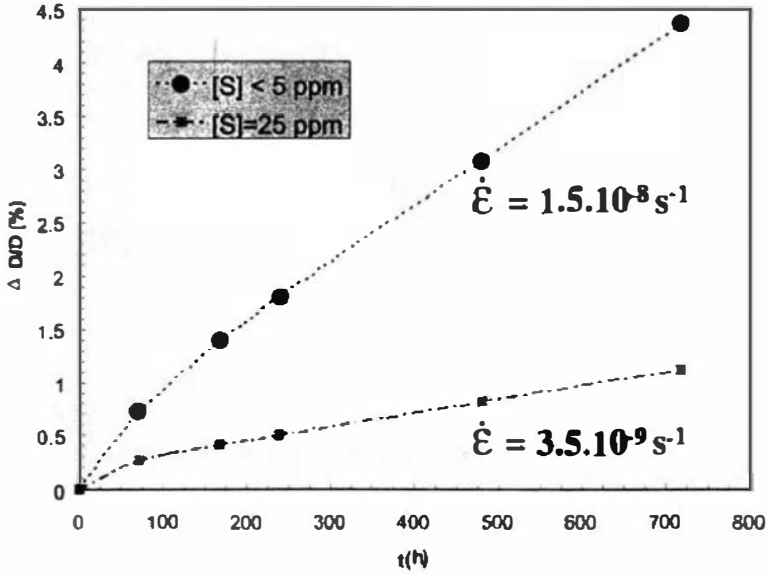


FIG. 1—*Variation of diametral creep strain with time in fully recrystallized Zr-1%Nb-0.13%O tubes under biaxial stress (circumferential stress = 130 MPa).*

## Experimental

### *Materials*

Two different alloys were used in the present study: α-zirconium specially supplied in the form of plates and an industrial alloy supplied in the form of tubes by Cézus Framatome ANP. Both materials show a strong rolling texture with the c axis perpendicular either to the rolling direction or to the tube axis (Fig. 2).

*α-Zirconium*—It was supplied in the form of hot rolled plates recrystallized at 650–700°C during 4 h. The resulting grain size is 45 μm, and there are few precipitates ($Zr_3Fe$). Different concentrations of sulfur and oxygen have been supplied, as reported in Table 1. The materials containing less than 5 ppm sulfur will be referred to as "low sulfur" (LS), and those with 25 ppm sulfur as "high sulfur" (HS). The same denomination will be used concerning oxygen content. Neither sulfur nor oxygen contents affect the microstructural parameters (grain size and texture).

*Zr-1%Nb-0.13%O Alloy*—The material was supplied in the form of tubes with a 9.5-mm outer diameter and 0.57-mm thickness. The tubes are produced by pilgering in five steps, using a process that allows the reduction of the diameter and the thickness in the same operation. After each rolling step, the tubes were degreased, chemically etched, and annealed at a temperature just below the $\alpha/(\alpha+\beta)$ equilibrium temperature, giving a total recrystallization. The aim of this procedure was to obtain fine β-Nb precipitates homogeneously distributed in the α–Zr matrix in order to have improved corrosion properties. The mean diameter of these spherical precipitates was in the range 40–60 nm, and their density was very low (about 120 per $mm^3$); the grain size was 4 μm. The chemical composition is given in Table 2; two different sulfur compositions were supplied with no noticeable effect on the microstructural parameters.

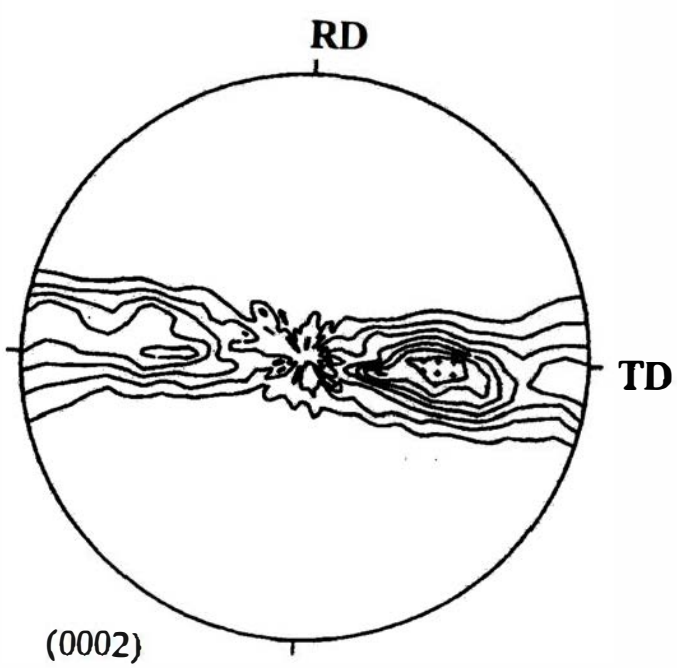


FIG. 2—*Typical rolling texture of the materials under study.*

### *Mechanical Tests*

In order to characterize the influence of the sulfur content on the mechanical properties of α-zirconium and Zr-1%Nb-0.13%O alloy, creep and constant strain rate tests have been performed.

*Creep Tests*—They were performed on Zr-1%Nb-0.13%O alloy tubes that were internally pressurized. The initially pressurized specimens were introduced in an electric furnace at room temperature and heated. The creep tests were performed in air or in vacuum conditions (better than $10^{-6}$ torr to avoid oxidation in order to be able to observe the surface of the sample after creep). After the test, the specimens were cooled inside the furnace. The temperature was regulated within ±3°C. The temperature and stress ranges investigated were respectively 350–430°C and 90–150 MPa.

The creep strain is defined as the relative variation $\Delta D/D$ of the tube outer diameter, where $D$ is the outer diameter and $\Delta D$ is the change in outer diameter. It was obtained as the mean value of several measurements performed with a laser micrometer: three different sections of the specimen, along six different generating lines. The accuracy of each measurement is ± 1 μm. During the primary creep stage, the samples were taken out from the furnace and measured every 72 h, until 240 h, and every 240 h after that time.

TABLE 1—*Chemical composition of α-zirconium materials.*

| Element | O | | Fe | Cr | H | Others | S | |
|---|---|---|---|---|---|---|---|---|
| Weight, ppm | 300 | 1200 | 130 | 30 | 10 | <50 | <5 | 25 |

TABLE 2—*Chemical composition of Zr-1%Nb-0.13%O materials.*

| Element | O | Nb | Fe | H | Others | S |
|---|---|---|---|---|---|---|
| Weight, ppm | 1200 | $1.01 \times 10^4$ | 108 | <5 | <50 | <5 |

25

The hoop stress in the tube wall is controlled by adjusting the inner pressure of the argon gas. Since $e << D_m$ ($e$ = tube thickness and $D_m$ = mean diameter), the radial stress can be safely neglected and the hoop $\sigma_{\theta\theta}$ and axial $\sigma_{zz}$ stresses assumed constant in the thickness:

$$\sigma_{\theta\theta} = \frac{PD_m}{2e} \quad \text{and} \quad \sigma_{zz} = \frac{PD_m}{4e} \tag{1}$$

where $P$ is the gas pressure inside the tube at the test temperature.

*Constant Strain Rate Tensile Tests*—Tensile tests were performed on α-zirconium specimens between room temperature and 500°C using an MTS machine equipped with a furnace. The temperature was controlled within ±2°C and the deformation was measured using an extensometer. The tests were carried out using crosshead velocity control but not with real strain rate control. Nevertheless, as soon as the plastic regime was reached, the strain rate became nearly constant. The crosshead velocity was adjusted so that the strain rate in the plastic regime was $5 \times 10^{-5} s^{-1}$.

The strain rate sensitivity was measured by performing strain rate increment tests at three levels: $5 \times 10^{-4} s^{-1}$, $5 \times 10^{-5} s^{-1}$, and $5 \times 10^{-6} s^{-1}$; some tests were also performed at very low strain rate ($10^{-8} s^{-1}$). All tests were performed on samples with the stress axis aligned with the rolling direction. On Zr-1%Nb-0.13%O alloys, the tests were performed on tubes between 270 and 430°C, using an Instron machine under a strain rate of $5 \times 10^{-5} s^{-1}$ in the plastic regime.

### *Microscopy*

Observations and characterizations of the deformation mechanisms have been performed using optical microscopy, Scanning Electron Microscopy (SEM), and Transmission Electron Microscopy (TEM); these techniques complemented each other.

*Surface Preparation*—The samples were electro-polished in a solution of 80% acetic acid and 20% perchloric acid at 20 V, at 7°C for 150 s. The resulting surface was suitable for the observation of the microstructure using SEM and optical microscopy.

*Thin Foil Preparation*—Strips ($3 \times 10$ mm$^2$) were cut from the tubes or from the flat specimens. They were mechanically polished with a 1200 grit paper to 150 μm thickness. The 3-mm-diameter disks were punched and electro-polished (70% methanol, 20% monobutylic ether, and 10% perchloric acid, 20 V, 30°C). When suitably thin, the specimens were washed in methanol.

The TEM studies of the thin foils were carried out using a CM30 Philips with a 300 kV accelerating voltage.

## Characterization of the Sulfur Effects

### *Creep Tests*

All creep tests have been performed on Zr-1%Nb-0.13%O alloy tubes. The sulfur effect was observed in all the temperature and stress ranges used: 350°C ≤ $T$ ≤ 430°C;

90 MPa $\leq \sigma \leq$ 130 MPa. Sulfur shortens the primary creep stage and lowers the secondary creep rate (Fig. 3). The ratio of the creep rates for the HS materials to the LS materials is about 3 and constant in the whole temperature and stress ranges.

If the steady-state creep regime is analyzed using the classical creep law:

$$\dot{\varepsilon} = \dot{\varepsilon}_0 \left(\frac{\sigma}{\mu}\right)^n \exp\left(-\frac{Q}{RT}\right) \tag{2}$$

then both the stress sensitivity ($n \cong 4$) and the apparent activation energy ($Q \cong 215$ kJ/mol) remain insensitive to sulfur concentration (Fig. 4*a* and *b*). It should be noted that a difference of only 6 kJ/mol ($Q^{HS} - Q^{LS} = 6$ kJ/mol) could explain the factor of 3 for the steady state creep rates. Since 6 kJ/mol is smaller than the uncertainty in the values of $Q$, the full effect of sulfur can be understood by postulating the dependence of the apparent activation energy in sulfur concentration. Nevertheless, the apparent activation energy is directly dependent on the controlling mechanism, and a different value of $Q$ would mean a different mechanism. However, such a small difference in their activation energy for two different mechanisms is not very plausible. Therefore, in the rest of this paper, $Q$ and the nature of the controlling deformation mechanism will be considered to be independent of the sulfur content. The only dependence of the sulfur content is on the kinetics of the controlling deformation mechanism.

*Constant Strain-Rate Tensile Tests*

*Zr-1% Nb-0.13% O Alloys*—Sulfur increases the value of the yield stress, the flow stress being always higher for HS than for LS materials (Fig. 5). This effect is stronger at 400°C than at 200°C. If the tensile curves are analyzed by means of the classical hardening law:

$$\sigma = A\varepsilon^p \tag{3}$$

it can be observed that the sulfur content does not affect the value of the strain hardening

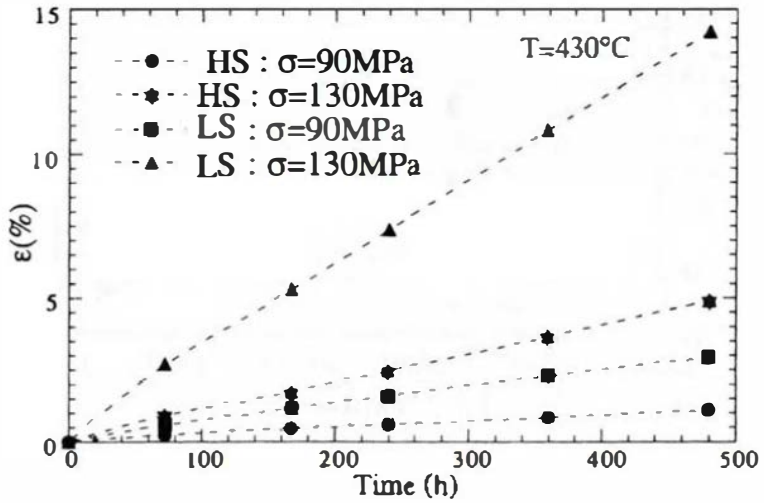


FIG. 3—*Creep curves for low and high sulfur Zr-1%Nb-0.13%-O alloys performed under internal pressure at T = 430°C.*

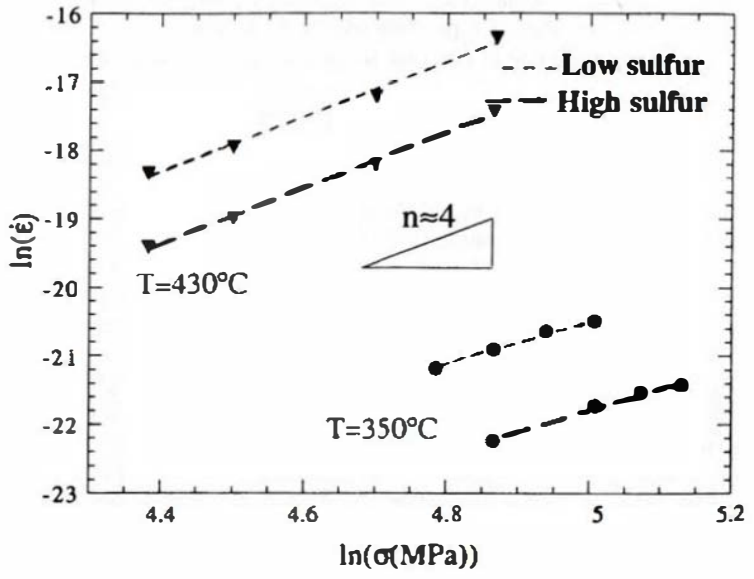


(a)

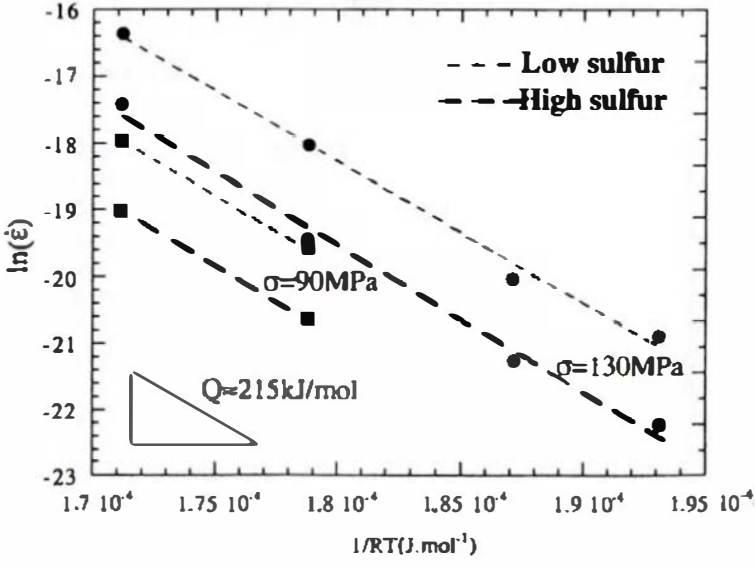


(b)

FIG. 4—*Creep behavior:* a) *Stress sensitivity,* b) *Apparent activation energy.*

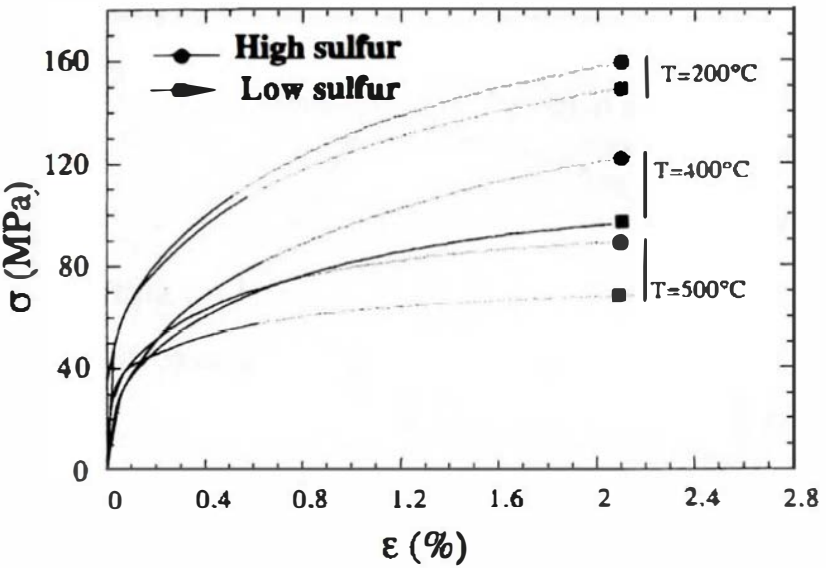


FIG. 5—*Stress-strain curves for low and high sulfur Zr-1%Nb-0.13%O alloys performed under different temperature conditions.*

exponent $p$, but increases $A$ (Table 3). Thus, the sulfur content shows an effect similar to a strain-rate effect. This analogy between sulfur content and strain-rate is clearly shown in Fig. 6, where the stress-strain curve of a HS material for a strain rate of $6 \times 10^{-6}s^{-1}$, and the curve of a LS material under $6 \times 10^{-5}s^{-1}$ are superimposed (see also boldfaces in Table 3). Then, following standard arguments, since $p$ is associated with the strain hardening mechanism, it can be deduced that sulfur does not affect the nature of this mechanism. The identity between the sulfur effect and a strain rate effect suggests that sulfur modifies the material viscosity; thus, instead of a modification of the deformation controlling mechanism, it seems that sulfur modifies the kinetics of the mechanism. This is consistent with the independence of the parameters ($n$, $\beta$) in the steady-state creep law on the sulfur concentration.

*α-zirconium*—The sulfur effect is in agreement with what was reported for Zr-1%Nb-0.13%O alloy here above. Since α-zirconium contains very few precipitates, this result shows that the sulfur effect is independent of precipitates. Nevertheless, it cannot be excluded that sulfur operates through a coupling with elements present in the two alloys as oxygen or iron.

TABLE 3—*Influence of sulfur content on the parameters of the hardening law* $\alpha = A\varepsilon_p$ *(Note the similarity of A and p values at a given temperature for HS material at low strain rates and LS material at high strain rates).*

| | | $T$ = 270°C | | $T$ = 350°C | | $T$ = 430°C | |
|---|---|---|---|---|---|---|---|
| | | $6 \times 10^{-5}s^{-1}$ | $6 \times 10^{-6}s^{-1}$ | $6 \times 10^{-5}s^{-1}$ | $6 \times 10^{-6}s^{-1}$ | $6 \times 10^{-5}s^{-1}$ | $6 \times 10^{-6}s^{-1}$ |
| $A$ (MPa) | HS | 485 | 434 | 515 | 480 | 367 | 304 |
| | LS | 417 | 379 | 453 | 412 | 300 | 270 |
| $p$ | HS | 0.23 | 0.21 | 0.25 | 0.24 | 0.20 | 0.18 |
| | LS | 0.20 | 0.19 | 0.24 | 0.23 | 0.18 | 0.18 |

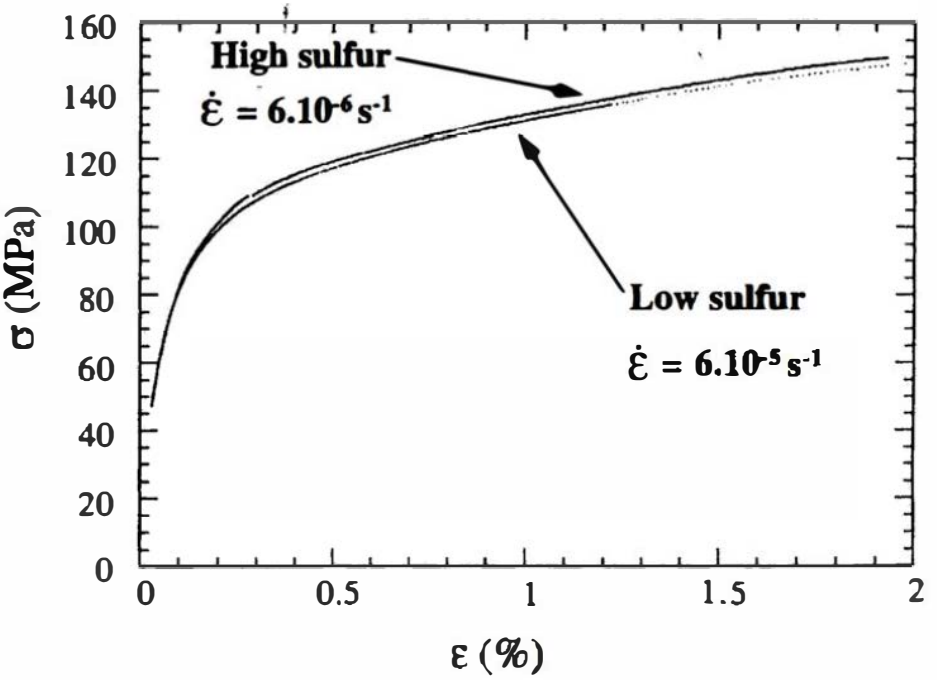


FIG. 6—*The viscous-like effect of sulfur (Zr-1%Nb-0.13%O; T = 430°C).*

The plot of the flow stress at 2% strain versus temperature shows the classical "athermal plateau" [2,3] between 250 and 400°C (Fig. 7*a*). The sulfur effect appears at about 100°C and increases up to 400°C; it accentuates the phenomenon, giving rise to an increase of the flow stress between 400 and 500°C.

The strain-rate sensitivity can be expressed as:

$$m = \left. \frac{\partial \ln \sigma}{\partial \ln \dot{\varepsilon}} \right|_T \tag{4}$$

Consistent with the above observations, the value of $m$ reduced by sulfur to almost zero between 350 and 400°C (Fig. 7*b*).

The apparent activation volume is:

$$V_a = kT \left. \frac{\partial \ln \dot{\varepsilon}}{\partial \sigma} \right|_T \tag{5}$$

which can be expressed in terms of $m$:

$$V_a = \frac{kT}{m\sigma} \tag{6}$$

The effective activation volume gives indications on the nature of the mechanism controlling the dislocation movement; it can be deduced from the apparent activation volume of the

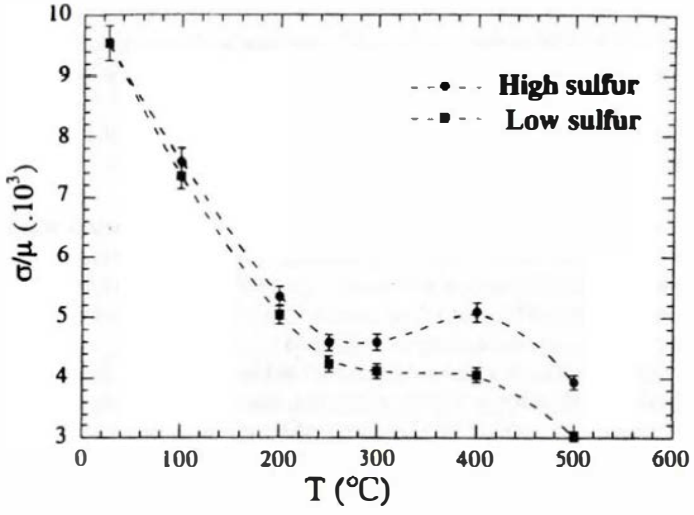


(a)

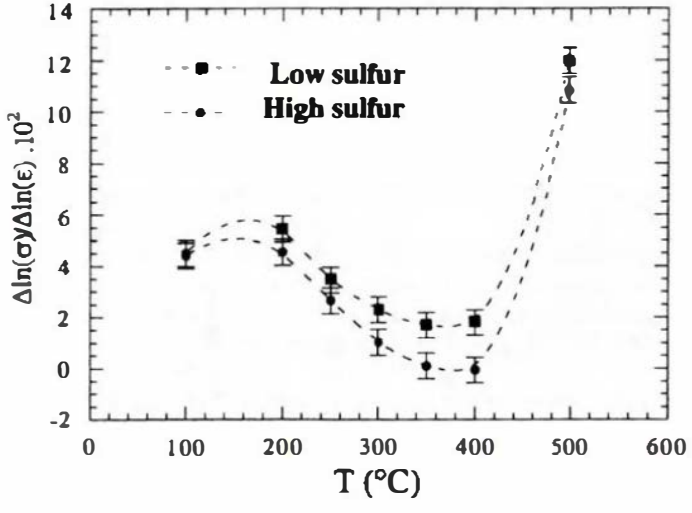


(b)

FIG. 7—*Effect of the sulfur content under constant strain-rate conditions:* a) *the athermal plateau* (*strain-rate* = $5 \times 10^{-5} s^{-1}$), b) *the strain-rate sensitivity.*

polycrystal by $V = MV_a$, where $M$ is the Taylor factor ($M = 4$ [2]). $V$ increases between 200 and 400°C:

- $T \leq 200$°C: $V \cong 40b^3$ a low value indicating that dislocations probably interact with short range or very dense obstacles (Peierls valleys, cross slip, concentrated solid solution. . .).
- $300 < T < 400$°C: $100 < V < 400b^3$ a value too high for dislocation climb as the controlling mechanism.

In some tests, after a certain amount of plastic strain, the specimen was unloaded and held at a fixed temperature for 30 min. When it was reloaded, the stress climbed beyond the previous flow stress, then dropped, and then followed the normal work-hardening curve. This is an age-hardening peak. The plot of the stress increment ($\Delta\sigma$) versus temperature shows that sulfur increases the age-hardening peak (Fig. 8).

The athermal plateau, the age-hardening peak, and the minimum in strain rate sensitivity are generally understood in terms of the interaction between dislocations and oxygen atoms based Shoeck-Seeger type models [4,5]. Since sulfur amplifies all these effects, the question of a coupling effect between sulfur and oxygen, or of a supplementary dynamical hardening due to sulfur, must be addressed. These points are discussed below.

## The Effectively Active Deformation Mechanisms

The potentially active deformation mechanisms in zirconium are documented [6-10]. Nevertheless, for all the potential mechanisms, we have to determine which of them are principally active, where and when they are activated, how their activation depends on the loading and temperature conditions and, above all, how sulfur modifies their activity. Using both

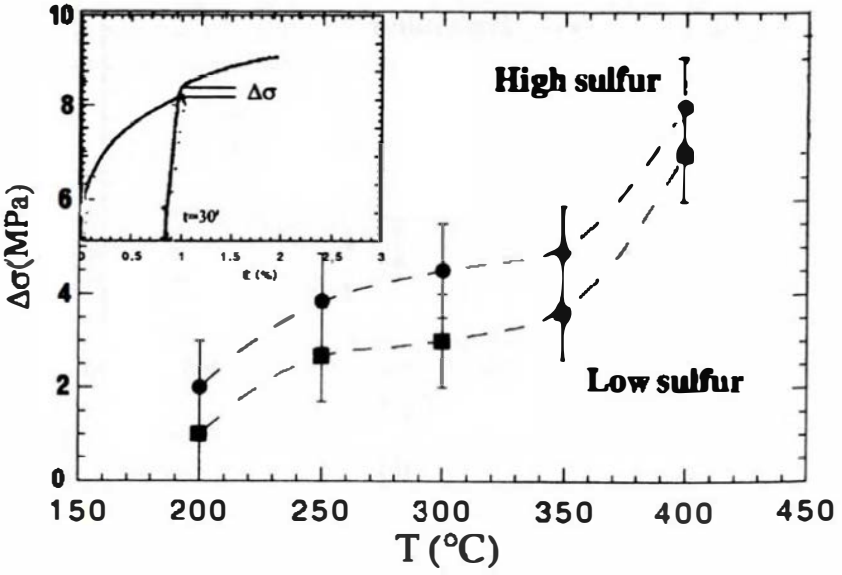


FIG. 8—*Effect of the sulfur content on age-hardening.*

SEM and TEM observations, these mechanisms have been characterized in the whole temperature and stress range and for HS and LS materials.

An essential conclusion is that no effect of sulfur content on the nature, occurrence, or density of the deformation mechanisms could be shown. Therefore, in the following, they are presented without reference to the sulfur content. The conclusions of the study of the deformation mechanisms are as follows.

Whatever the deformation mode, no twins were observed by either SEM or by TEM; the only active deformation mechanism is plastic glide. Two temperature domains must be considered:

- $T < 200$°C: The only slip systems are of the prismatic type (Fig. 9*a*) with a very small amount of pyramidal glide. Only long screw <a> type dislocations (proof of a high Peierls friction) can be observed; in most grains, two of the three possible prismatic slip systems were activated (sometimes three) and showed a homogeneous distribution (Fig. 9*b*). The dislocations of the different slip systems interact; if the interaction is attractive, they form junctions; if it is repulsive, they cross and yield sessile jogs that are responsible for the formation of long dipoles.
- $T > 200$°C: Prismatic glide is still dominant (80%), but first-type pyramidal glide is more frequent (10%) and cross slip, from the prismatic planes towards the pyramidal ones, can be observed (Fig. 10*a*). The dislocations are bent in pyramidal planes (Fig. 10*b*) showing that their movement is no more controlled by Peierls friction. Neither pile-ups nor cells are formed, the dislocations being homogeneously distributed inside the grains.[6]

## Origin of the Sulfur Effect

The effect of sulfur on the mechanical behavior of α-zirconium and Zr-1%Nb-0.13%● alloy is confirmed, but its origin is still not explained. Sulfur does not modify the microstructure (grain size, texture, precipitates, . . .), nor the nature of the deformation controlling mechanism. It seems to modify the kinetics of that mechanism but not the mechanism itself. Moreover, it must be kept in mind that this strong effect is due to a very small amount of sulfur. In the following, an attempt is made to identify at what scale and through which defects sulfur can affect the deformation kinetics.

Using all the previous observations, a limited list of potential controlling mechanisms was prepared (Table 4). Each of these mechanisms needs the activity of one elementary phenomenon that involves one type of defect. Thus, the influence of sulfur on the deformation kinetics is the consequence of the interaction of sulfur atoms, alone or associated with other solute atoms, with the relevant defects.

In the following, the relevance of these elementary phenomena is analyzed to attempt to shorten the list and point out which sulfur/defect interaction is the most reliable.

[6] The observations reported in Fig. 10 could appear contradictory since most of the slip lines correspond to the activity of prismatic glide and the observed dislocations are in pyramidal planes. The slip lines are the traces left by a great number of dislocations that have glided mainly in prismatic planes. The observed dislocations are those remaining after cooling the material under load. Since these two observations must be consistent, they show that above 200°C dislocations glide easily in prismatic planes and with more difficulty in pyramidal ones.

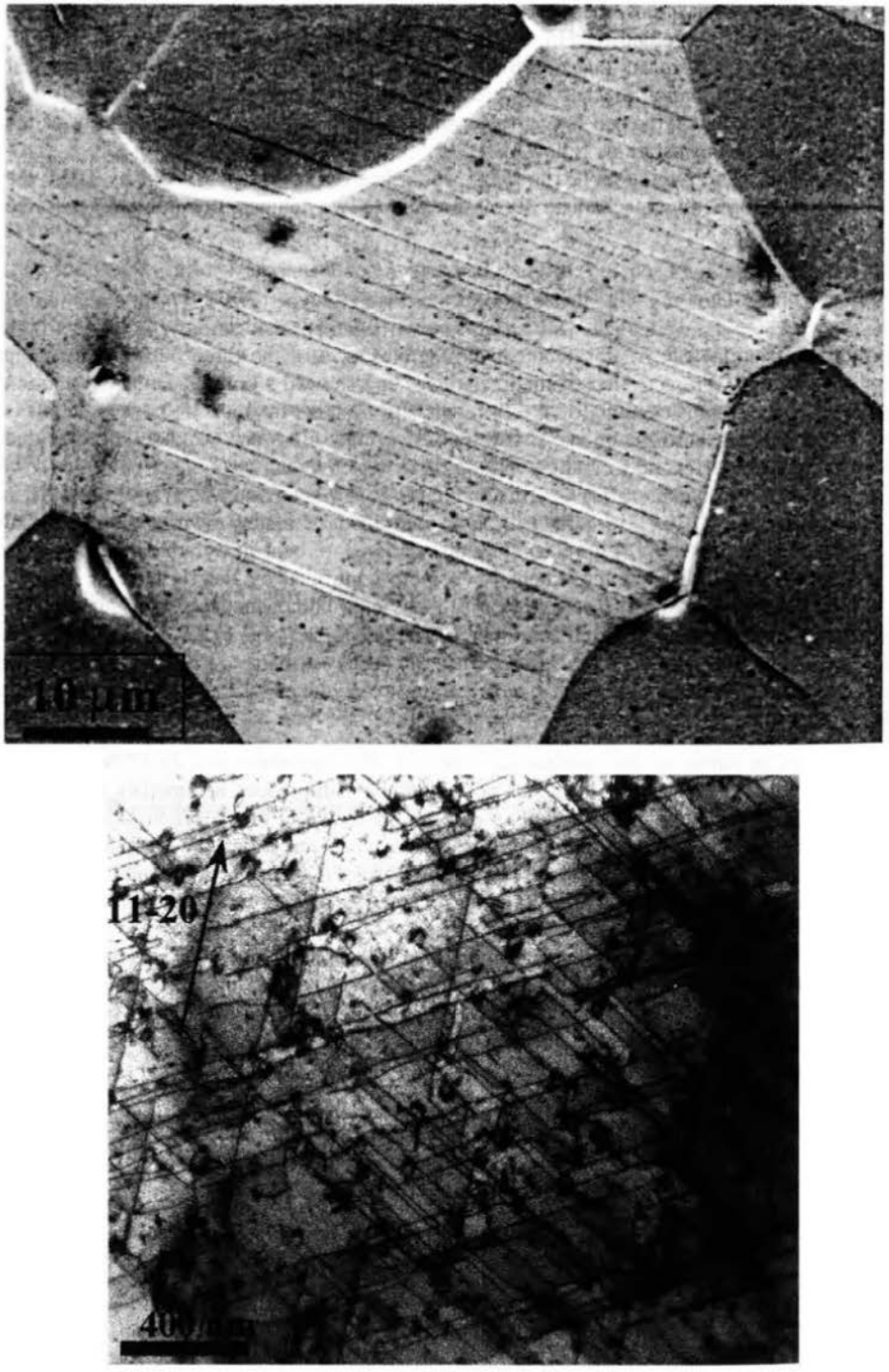


FIG. 9—*Deformation mechanisms at T < 200°C:* a) *prismatic slip plane traces (SEM),* b) *long screw <a> type dislocations (TEM: basal projection).*

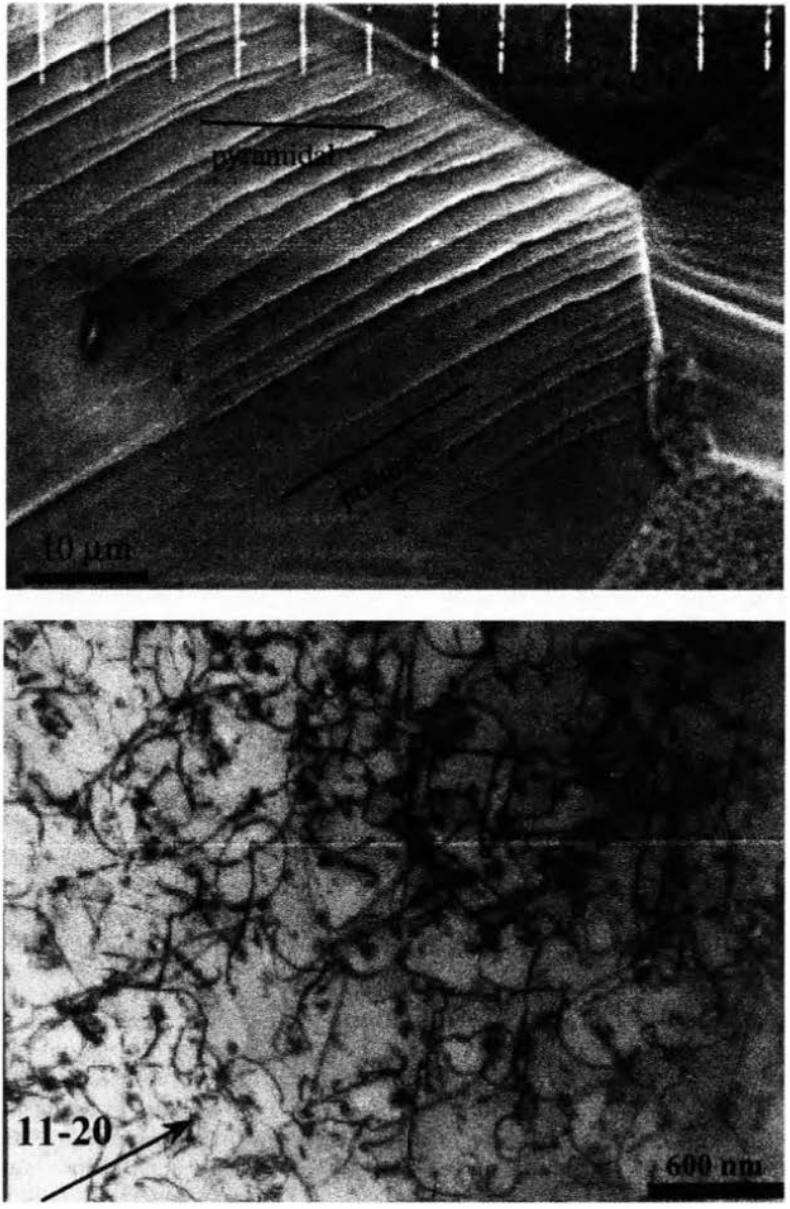


FIG. 10—*Deformation mechanisms at T > 200°C: a) prismatic slip plane traces with some pyramidal plane traces suggesting cross-slip events (SEM), b) <a> type dislocations bent in pyramidal planes (TEM; basal projection).*

TABLE 4—*The potential controlling mechanisms and the associated defects.*

| Potential Controlling Mechanism | Elementary Phenomenon | Defect |
|---|---|---|
| Relaxation of intergranular incompatibilities | Grain boundary sliding | Grain boundary |
| Restoration by dislocation climb and annihilation | Bulk self-diffusion | Vacancy |
| | Pipe self-diffusion | Dislocation |
| Sessile jog dragging | Bulk self-diffusion | Vacancy |
| | Pipe self-diffusion | Dislocation |
| Dislocation glide | Peierls friction | Dislocation |
| Restoration by cross-slip and annihilation | Cross-slip | Dislocation |

*Grain Boundary Sliding*

Using a microgrid technique [*11*], it has been verified that grain boundary sliding was not observed at any temperature or strain rate neither for HS nor LS materials. Thus, grain boundary sliding is not a deformation mechanism. This does not mean that it is not the controlling mechanism, since a very small amount of sliding could relax the intergranular incompatibilities.

In order to check this hypothesis, three materials with different grain sizes have been obtained by critical working and recrystallization of α-zirconium. The grain sizes are 45 μm (original small grain material referred to as SG), 200 μm (medium grain material referred as MG), and 800 μm (large grain material referred to as LG); the texture and composition of the three materials are identical.

Under constant strain-rate tensile test conditions, the flow stress at 1% strain shows a classical Hall-Petch behavior (Fig. 11):

(7)

where $\Phi$ is the grain size and $\sigma_0$ the single crystal flow stress. HS and LS materials exhibit the same $k$ value, whereas $\sigma_0$ is strongly affected. Thus, sulfur only affects the intragranular behavior, which leads to the conclusion that grain boundary sliding is not the controlling mechanism. Therefore, sulfur/grain boundary interaction is not the origin of sulfur effect.

*Self-Diffusion*

The interpretation of creep is classically associated with self-diffusion. This phenomenon can control two different types of mechanisms:

a) Deformation by pure diffusion (Nabarro-Herring or Coble mechanism),
b) Dislocation climb or sessile jog dragging.

The pure diffusion hypothesis is unlikely in the investigated temperature range; moreover, this phenomenon gives a stress sensitivity factor of 1, which is very different from the value of 4 we have measured. Thus, pure diffusion can be rejected.

The second hypothesis of a dislocation climb mechanism controlled by bulk or pipe diffusion needs more attention. The creep activation energy value is classically associated with the controlling phenomenon. Many authors have measured a value close to the bulk diffusion

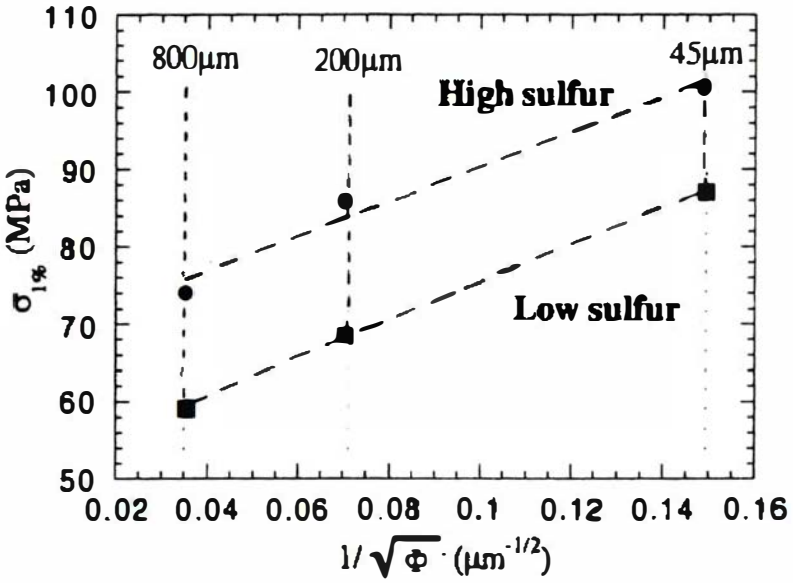


FIG. 11—*Effect of sulfur on the Hall-Petch type behavior (strain-rate = 5 × 10⁻⁵s⁻¹; T = 400°C; αZr).*

activation energy and they have concluded that creep is controlled by bulk self-diffusion [*12–14*]. The dislocation creep models consider that dislocations climb to overcome obstacles whatever their nature (precipitates, pile-ups. . .) and then glide freely between the obstacles; therefore, we conclude that the deformation kinetics is controlled by the time necessary to get over obstacles; this time is controlled by self-diffusion.

Such a model suggests a law of the form [*15*]:

$$\dot{\varepsilon} = A \frac{\mu b}{kT} D_v \left(\frac{\sigma}{\mu}\right)^n \tag{8}$$

with

$$D_v = D_0 \exp -\frac{Q_v}{kT}$$

where $A$ is a constant depending of the microstructure ($1 < A < 100$), $\mu$ the shear modulus, $\sigma$ the applied stress, $n$ the stress sensitivity factor, $D_v$ is the bulk self-diffusion coefficient, and $Q_v$ the bulk self-diffusion activation energy.

Only $A$ and $n$ depend on the microscopic details of the model. The Zr-1%Nb-0.13%O alloy steady state creep behavior can be analyzed with $n = 4$ and $Q = 215$ kJ/mol. This can suggest a dislocation climb-controlled mechanism. Equation 8 suggests the comparison of the apparent activation energy $Q$ for creep and the bulk self-diffusion activation energy $Q_v$.

There is large scatter in the available $Q_v$ values: 90, 217, 306 kJ/mol according to Gruzin [*16*], Lyashenko [*17*], and Hood et al. [*18*], respectively. Many authors [*19–21*] have suggested that, for temperatures lower than 850°C, diffusion could occur both by bulk and pipe diffusion. In general, pipe diffusion has an activation energy value about half the value for bulk diffusion and plays a predominant role at lower temperatures. Thus, diffusion measure-

ments at 850°C could be affected by the dislocation density, and probably be underestimated; this could explain the low values reported by Gruzin and Lyashenko. Finally, Hood et al. give a mean value for the bulk self-diffusion coefficient [18]:

$$D_v = 9.0 \times 10^{-5} \exp \frac{-3.17 \pm 0.04 \text{ eV}}{kT} \text{ m}^2 \cdot \text{s}^{-1} \quad (9)$$

This equation was derived from different experiments, all performed at temperatures higher than 600°C. No value is available for $T = 400$°C.

The creep activation energy we measured (215 kJ/mol) is significantly lower than the value given by Hood et al. (306 kJ/mol), leading to the conclusion that bulk self-diffusion is not the creep-controlling mechanism for $T < 400$°C. Nevertheless, it is risky to select a controlling mechanism on the basis of the activation energies only, because the relation between activation parameters and mechanisms is far from one-to-one [22]. In order to evaluate the possibility of a bulk self-diffusion controlled mechanism, we have used Eqs 8 and 9 to estimate the resulting strain rate. At 400°C the diffusion coefficient value is $D_v = 1.7 \times 10^{-28} \text{m}^2\text{s}^{-1}$. Under a stress of 130 MPa and for $A = 10$, the calculated strain rate is $10^{-14}\text{s}^{-1}$, i.e., much lower than the experimental one ($1.5 \times 10^{-8}\text{s}^{-1}$). This seven orders of magnitude cannot be due to the model. The main cause for that discrepancy is the value for the bulk self-diffusion coefficient that is too low.

In conclusion, all these observations allow the discarding of bulk self-diffusion as the controlling mechanism in the temperature range of interest. But mechanisms implicating pipe self-diffusion remain plausible. Nevertheless, the activation volumes measured between 300 and 400°C are always higher than $100b^3$, thus excluding dislocation climb mechanisms since their activation volume is of the order of $b^3$. The only diffusion-controlled mechanism that cannot be discarded is jog dragging controlled by pipe diffusion.

*At this stage we can draw the following partial conclusions:*

a) *two sulf interaction types can be dismissed: sulfur/grain boundary and sulfur/vacancy*
b) *sulfur interacts with dislocations and the mechanism controlling the deformation kinetics is a dislocation mechanism.*

*Then two questions naturally arise:*

- *does sulfur behave as an immobile obstacle pinning dislocations?*
- *does sulfur form a mobile cloud slowing down the dislocation movement?*

*Sulfur/Dislocation Interaction*

*Is Sulfur a Fixed Obstacle?*—Two types of models have been derived to describe the interaction between dislocations and fixed point defects:

- *models for bcc materials with a large Peierls friction in which point defects interact with double kinks [23,24]*
- *models for fcc materials in which point defects act as pinning points [25,26].*

In zirconium, when $T < 200$°C, we have shown that deformation is controlled by the movement of long <a> type screw dislocations subject to a high Peierls stress: then, the

first type of model could be applied to this temperature range. When $200 < T < 500$°C, the observed long curved dislocation suggest that Peierls friction is no longer active; the second type of model would then be pertinent.

All of these models predict a hardening decrease with increasing temperature, whereas in the case of zirconium/sulfur interaction, the effect appears around 100°C and is at a maximum value around 400°C. Moreover, predictions of hardening by these models, on the basis of an overestimated sulfur/dislocation interaction energy (1 eV), give values ranging between 0.1 and 1 MPa, when the experimental value is 25 MPa. This discrepancy is due to the very low sulfur concentration. Therefore, these models cannot explain the observations. *We conclude that sulfur is mobile.*

Sulfur amplifies many effects reputed to be due to oxygen: a dynamical strain-aging plateau, drop in strain rate sensitivity, and static aging peak. Thus, it is justified to compare sulfur and oxygen effects and try to understand whether they are coupled or independent.

### *Are the Oxygen and Sulfur Effects Independent?*

Dynamical strain-aging effects express themselves in precise ranges of temperatures and strain rates. In particular, they disappear when the temperature is too high or the strain rate too low [*27–29*].

At a $5 \times 10^{-5}s^{-1}$ strain-rate, the sulfur effect appears at 100°C and is at a maximum value around 400°C. Very low strain-rate tests ($2 \times 10^{-8}s^{-1}$) performed on HS and LS materials (Fig. 12*a*) show a sulfur hardening of 25 MPa at 1% strain, similar to that obtained at $5 \times 10^{-5}s^{-1}$.

The same experiment has been performed on HS and LS materials, but with an oxygen content of 300 ppm. The same hardening amount of 25 MPa was observed (Fig. 12*b*). Thus, the sulfur effect is independent of decreasing the oxygen concentration; nevertheless, the oxygen concentration remains too high (10 times higher than sulfur amount) to be able, from this experiment, to exclude interactions between oxygen and sulfur. Now, if Figs. 12*a* and *b* are superposed (Fig. 13), it appears that the oxygen effect disappears at low strain-rate, whereas the sulfur effect remains unchanged. Therefore, we can conclude that:

- the sulfur and oxygen effects are independent,
- the nature of these two effects is different.

Thus, the sulfur effect can be considered as intrinsic, since it is not a simple amplification of the oxygen effect. A complex defect (S/O or S/Fe) could be the effectively active defect; tests performed on high purity zirconium with controlled amounts of impurities are necessary to determine the nature of the active defect.

*In order to explain the very strong effect of a very low concentration of sulfur persisting at low strain rates, we are led to formulate a new hypothesis; that is, sulfur could segregate at dislocation cores and modify their structure.*

### *Segregation of Sulfur at Dislocation Cores*

Legrand [*30,31*] has studied the structure of the core of <a> type screw dislocations using a tight-binding model, which takes into account the partial filling corresponding to titanium and zirconium of the electronic *d* band. The core is mainly spread in the prismatic plane explaining the easy prismatic glide, but shows also secondary spreading in the basal plane. It follows that the movement in the prismatic plane requires that these basal components must constrict.

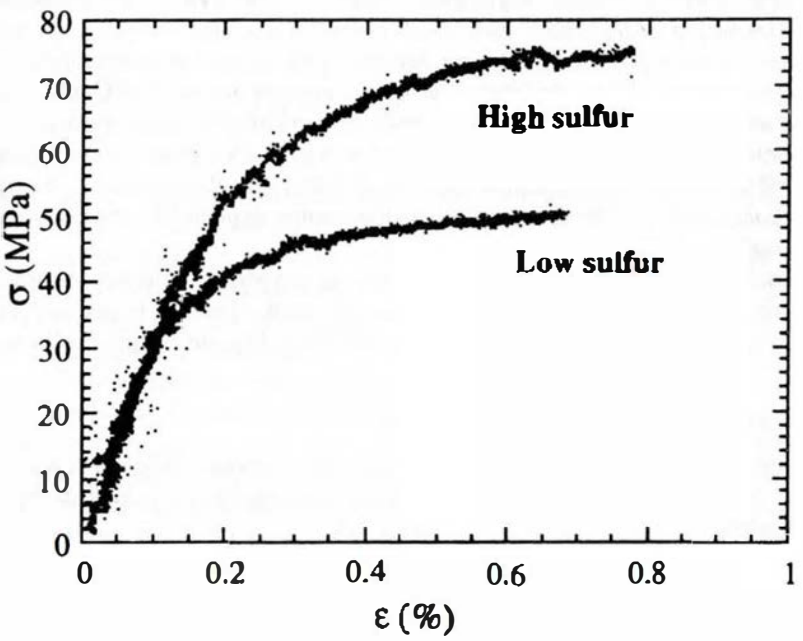


(a)

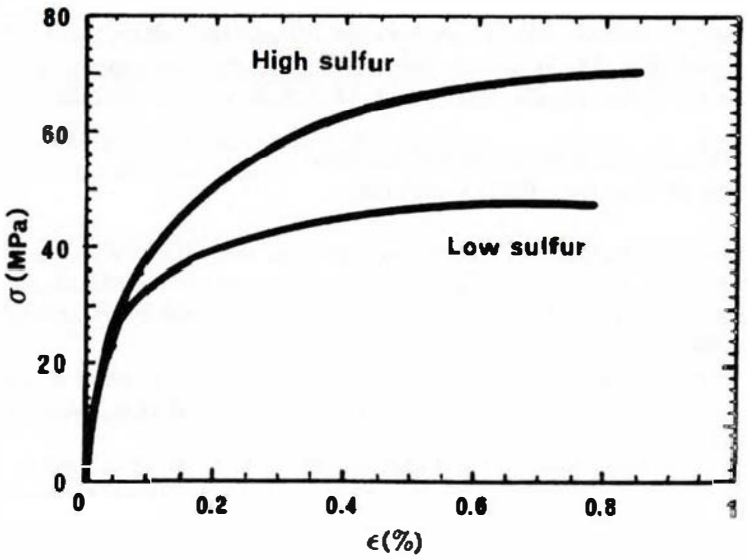


(b)

FIG. 12—*The sulfur effect persists at low strain-rate ($5 \times 10^{-8} s^{-1}$; T = 400°C), as well for both:* a) *a high oxygen content (1200 ppm),* b) *a low oxygen content (300 ppm).*

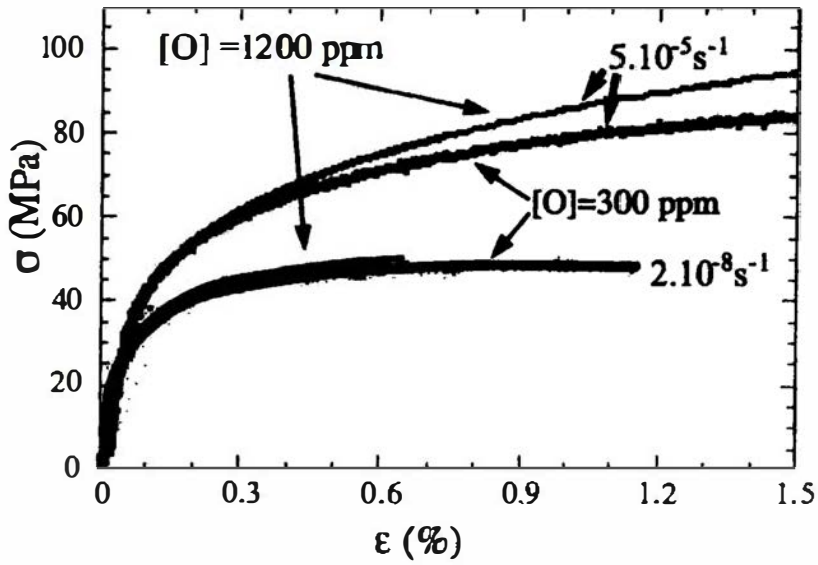


FIG. 13—*The hardening e of oxygen disappears at low strain-rate (low sulfur material; T = 400°C).*

Sulfur segregation at dislocation cores could modify this structure, which would affect most of the properties of these dislocations: Peierls friction, cross slip, pipe diffusion, interaction with other impurities, etc. . . The persistence of sulfur hardening at low strain-rates can be explained, as well as the "viscous" sulfur effect. This hypothesis is consistent with all the experimental observations.

Atomic scale numerical simulations have been performed in order to check the validity of this hypothesis.

*Atomic Scale Simulations*

Several experimental techniques, *a priori* pertinent to verify the effectiveness of sulfur segregation inside dislocation cores, have been considered.

High resolution TEM allows the observation of dislocation cores. Nevertheless, a perfect screw dislocation cannot be imaged by that technique, since its Burgers vector is normal to the image plane. A spread screw core could be imaged, due to its nonscrew components, but since they are very weak, the task was quite hazardous. Because of this difficulty, it was not attempted.

The atom probe performs analysis atom by atom; it could give the atomic composition of the dislocation core. But a sulfur atom is half the weight of a zirconium atom and a zirconium ion ($Zr^{4+}$) has a charge twice that of a sulfur ion ($S^{2+}$); thus, the time of flight of both ions is quasi-identical, so that the signals would be very difficult to distinguish.

To avoid these difficulties, atomistic simulations were used. They were performed by combining simulations based on semiempirical interatomic potentials [*32*] and *ab initio* electronic structure calculations, performed in the framework of the density functional theory in the local density approximation. For the latter, the PWSCF plane-wave pseudo-potential code [*33*] was used. The details of this work will be reported elsewhere; the results that are most pertinent to the discussion on the hypothesis of a sulfur segregation at dislocation cores are summarized here.

The preferential bulk site for the dissolution of sulfur was first investigated by *ab initio* calculations, by comparing the energies of various relaxed configurations. It was determined that sulfur, like oxygen, is an interstitial rather than a substitutional impurity, and that it is most favorable in the octahedral site. Moreover, sulfur atoms are shown to induce important distortions in the zirconium lattice, as attested by the large increase of the volume of the octahedral site ($\Delta V/V = 30\%$), whereas the lattice is weakly affected by oxygen atoms ($\Delta V/V = 1\%$).

The dislocation simulations were performed in two steps. First, the structure in a large supercell was relaxed using a semiempirical interatomic potential for zirconium [*32*]. In agreement with previous calculations [*31,34*] it was found that, within this simplified approach, the <a> type screw dislocation is more stable when the core is spread in the basal plane, in disagreement with both experiments and more accurate calculations. However, the configuration with the core spread in the prismatic plane and with secondary spreading in the basal plane—as it should—is found to be *metastable* [*34*], which allows calculations on this correct configuration to be carried out. By examining the displacement of such a dislocation, it was found that the glide in the prismatic plane is, in fact, a zig-zag glide in first type pyramidal planes (Fig. 14). This glide mechanism could be at the origin of non-Schmidt law effects reported in titanium and suspected in zirconium.

The *ab initio* calculations were then performed by extracting the positions of the 37 atoms closest to the dislocation core (Fig. 15). The atoms at the outer layer were kept fixed, and the other atoms were allowed to relax. The maximum cancellation of errors was ensured by performing bulk and dislocation calculations with the same geometry. At least three sites close to the core with a negative segregation energy of the order of −0.1 eV have been identified. This attractive impurity/dislocation interaction is confirmed by doubling the cell dimension along the dislocation line. These sites are octahedral-like, but they have no equivalent in the bulk. Sulfur atoms affect the core structure of the dislocation, but our calculations at present do not allow quantifying the consequences of the distortions on dislocation mobility. The value of −0.1 eV can be regarded as rather large in absolute value, when compared to the "core" energy, i.e., the energy difference between cells with and without dislocations, which is only 0.5 eV/<a>. The impurity/dislocation interaction is, therefore, expected to be even more attractive if cells with larger dimensions perpendicular to the dislocation line are considered. Finally, finite temperature effects may also be crucial.

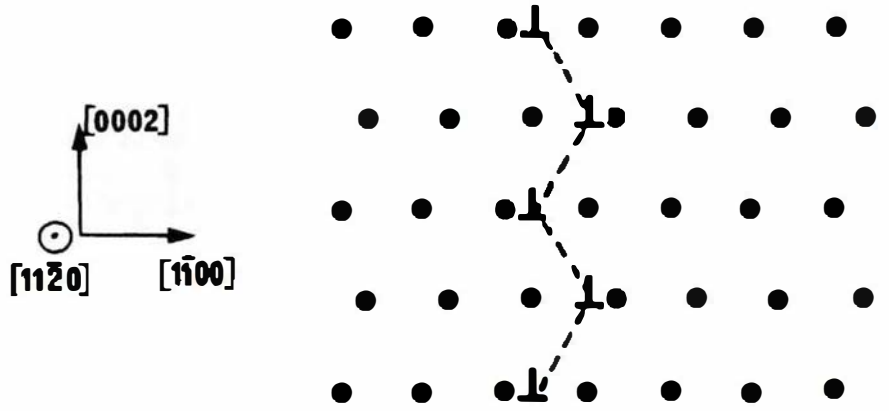


FIG. 14—*Schematic representation of the zig-zag motion of an <a> type screw dislocation (represented by ⊥) gliding in the prismatic plane.*

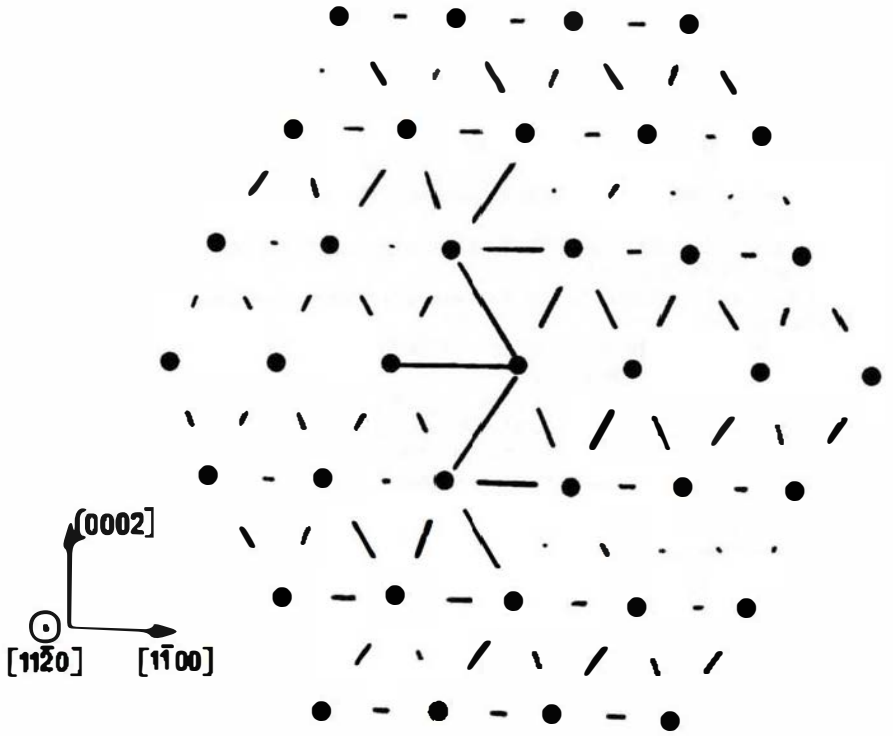


FIG. 15—*Projection in the [0001] direction of the atomic positions in the 37-atom cell used for the ab initio calculations of the core of the <a> type screw dislocation in α-Zr. The length of the segments between atomic sites is proportional to the relative displacement along the [0001] direction of the corresponding atoms.*

The present calculations are, therefore, consistent with the hypothesis of sulfur segregation at <a> type dislocation cores.

## Conclusion

The hardening effect of some ten ppm sulfur on the mechanical behavior of zirconium alloys has been clearly demonstrated. It appears at about 100°C and is at a maximum value around 400°C with a stress increment of 25 MPa under constant strain-rate conditions or a strain-rate decrease of a factor of three under constant stress conditions.

The nature of the deformation mechanisms is not affected since $Q$, $n$, and slip systems are unchanged and only their kinetics is modified: the sulfur effect is viscous-like. The sulfur effect has similarities to the oxygen hardening effect, but it has been demonstrated that it occurs by a different mechanism probably involving a modification of dislocation cores.

## References

[1] Charquet, D., Senevat, J., and Marcon, J. P., "Influence of Sulfur Content on the Thermal Creep of Zirconium Alloy Tubes at 400°C," *Journal of Nuclear Materials*, Vol. 255, 1998, pp. 78–82.

[2] Derep, J. L., Ibrahim, S., Rouby, D., and Fantozzi, G., "Deformation Behavior of Zircaloy-4 between 77 and 900 K," *Acta Metallurgica*, Vol. 28, 1980, p. 607.

[3] Ramaswani, B. and Craig, G. B., "Thermally Activated Deformation of Alpha Zirconium," *Transactions of the Metallurgical Society of AIME*, Vol. 239, 1967, p. 1226.
[4] de Paule E Silva, E., Com-Nougué, J., Béranger, G., and Lacombe, P., "Relation entre la cinétique de vieillissement après déformation du zirconium-α et la diffusion anisotrope de l'oxygène à courte distance," *Scripta Metallurgica*, Vol. 25, 1971, p. 795.
[5] Shoeck, G. and Seeger, A., "The Flow Stress of Iron and its Dependence on Impurities," *Acta Metallurgica*, Vol. 7, 1959, p. 469.
[6] Rapperport, E. J., "Room Temperature Deformation Processes in Zirconium," *Acta Metallurgica*, Vol. 7, 1959, p. 254.
[7] Akhtar, A. and Teghtsoonian, A., "Plastic Deformation of Zirconium Single Crystals," *Acta Metallurgica*, Vol. 19, 1971, p. 655.
[8] Sokurskii, I. N. and Protsenko, L. N., "Deformation Systems of α-zirconium," *Sov. J. At. Energy*, Vol. 4, 1958, p. 579.
[9] Bailey, J. E., "Electron Microscope Studies of Dislocations in Deformed Zirconium," *Journal of Nuclear Materials*, Vol. 7, 1962, p. 300.
[10] Crépin, J., Bretheau, T., and Caldemaison, D., "Plastic Deformation Mechanisms of β Treated Zirconium," *Acta Metall. Mater.*, Vol. 43, 1995, pp. 3709–3719.
[11] Allais, L., Bornert, M., Bretheau, T., and Caldemaison, D., "Experimental Characterization of the Local Strain Field in a Heterogeneous Elastoplastic Material," *Acta Metall. Mater.*, Vol. 42, 1994, pp. 3865–3880.
[12] Kim, Y. S., "Generalized Creep Model of Zircaloy-4 Cladding Tubes," *Journal of Nuclear Materials*, Vol. 250, 1997, p. 164.
[13] Kudlacek, L. and Hamersky, M., "Stress Characteristics of Creep of Alpha-Zr in the Temperature Interval 300–900 K," *Czech. J. Phys.*, Vol. B27, 1977, p. 738.
[14] Bernstein, L. M., "Diffusion Creep in Zirconium and Certain Zirconium Alloys," *Transactions of the Metallurgical Society of AIME*, Vol. 239, 1967, p. 1519.
[15] Spingarn, J. R., Barnett, D. M., and Nix, W. D., "Theoretical Descriptions of Climb Controlled Steady State Creep at High and Intermediate Temperatures," *Acta Metallurgica*, Vol. 27, 1979, p. 1549.
[16] Gruzin, P. L., Emelyanov, V. S., Ryabova, G. G., and Fedorov, G. B., *Second International Conference, Peaceful Uses of Atomic Energy*, Geneva, Vol. 19, 1958, p. 187.
[17] Lyashenko, V. S., Bykov, V. N., and Pavlinov, L.V., *Physics of Metals and Metallography*, New York, Vol. 8, No. 3, 1960, p. 40.
[18] Hood, G. M., Zou, H., Schultz R. J., Matsuura, N., Roy, J. A., and Jackman, J. A., "Self and Hf Diffusion in α-Zr and in Dilute Fe-Free Zr(Ti) and Zr(Nb) Alloys," *Defect and Diffusion Forum*, Vols. 143–147, 1997, p. 49.
[19] Naik, M. C. and Agarwala, R. P., "Self and Impurity Diffusion in Alpha Zirconium," *Acta Metallurgica*, Vol. 15, 1967, p. 1521.
[20] Marzocca, A. J. and Povolo, F., "Self-Diffusion Coefficient of α-zirconium," *J. of Mat. Sci. Letters*, Vol. 6, 1987, p. 431.
[21] Hood, G. M. and Schultz, R. J., "Trace Diffusion in α-Zr," *Acta Metallurgica*, Vol. 22, 1974, p. 459.
[22] Poirier, J. P., "Plasticité à haute température des solides cristallins," Editions Eyrolles, Paris, 1976.
[23] Dorn, J. E. and Rajnak, S., "Nucleation of Kink Pairs and the Peierls Mechanism of Plastic Deformation," *Transactions of the Metallurgical Society of AIME*, Vol. 230, 1964, p. 1052.
[24] Suzuki, H., "Solid Solution Hardening in Body-Centered Cubic Alloys," *Dislocations in Solids*, North Holland Publishing Company, 1979.
[25] Fleisher, R. L., "Rapid Solution Hardening, Dislocation Mobility and the Flow Stress of Crystals," *Journal of Applied Physics*, Vol. 33, No. 12, 1962, p. 3504.
[26] Friedel, J., "Dislocations," Pergamon Press, Paris, 1964.
[27] Conrad, H., "Effect of Interstitial Solutes on the Strength and Ductility of Titanium," *Prog. in Mater. Sci.*, Vol. 26, 1981, p. 123.
[28] Adda, Y., Dupouy, J. M., Philibert, J., and Quéré, Y., Eléments de métallurgie physique, CEA-INSTN Collection Enseignement, 1991, p. 1489.
[29] Strudel, J. L., "Interaction des dislocations avec des impuretés mobiles," Dislocations et déformation plastique, Yravals, Les Editions de Physique, 1979, p. 199.
[30] Legrand, B., "Relation entre la structure électronique et la facilité de glissement dans les métaux hexagonaux compacts," *Phil. Mag. B*, Vol. 49, No. 2, 1984, p. 171.
[31] Legrand, B., "Structure de cœur des dislocations vis 1/3<11-20> dans le titane," *Phil. Mag. A*, Vol. 52, No. 1, 1985, p. 83.

[32] Willaime, F. and Massobrio, C., "Development of an N-body Interatomic Potential for hcp and bcc Zirconium," *Phys. Rev. B*, Vol. 43, 1991, p. 11653.
[33] Baroni, S., Dal Corso, A., de Gironcoli, S., and Giannozzi, P., http://www.pwscf.org
[34] Girshick, A., Bratkovsky, A. M., and Vitek, V., "Atomistic Simulations of Titanium II Structure of 1/3<-12-10> Screw Dislocations and Slip Systems in Titanium," *Phil. Mag. A*, Vol. 77, No. 4, 1998, p. 981.